

Gap opening in graphene by simple periodic inhomogeneous strain

I.I. Naumov and A.M. Bratkovsky

Hewlett-Packard Laboratories, 1501 Page Mill Road, Palo Alto, California 94304

(Dated: October 24, 2018)

Using ab-initio methods, we show first that the *uniform* deformation either leaves graphene (semi)metallic or opens up a small gap yet only beyond its mechanical breaking point, contrary to claims in the literature based on tight-binding (TB) calculations. It is possible, however, to open up a global gap by a *sine-like* inhomogeneous deformation applied along any direction but the armchair one, with the largest gap along the zigzag direction (~ 1.0 eV) and without any electrostatic gating. The gap opening has a threshold character with very sharp rise when the ratio of the amplitude A and the period of the sine wave deformation λ exceeds $(A/\lambda)_c \sim 0.1$ and the inversion symmetry is preserved, while it is threshold-less when the symmetry is broken. The gap opening occurs in graphene mesh on boron-nitride substrate.

PACS numbers: 73.22.Pr, 81.05.ue, 62.25.-g

I. INTRODUCTION

Graphene, a hexagonally packed single layer of carbon atoms¹, is considered a strong candidate for post-silicon electronic devices. To meet this expectation, however, it is crucial to be able to open up a band gap at the Fermi level, which exists in silicon and is necessary for a switchable device. Since graphene has outstanding mechanical properties and capable of sustaining huge atomic distortions^{2,3} up to about 27%⁴ it becomes very interesting to use strain as a tool to introduce a band gap in graphene.

The idea of strain-induced band gap has been theoretically explored by Pereira *et al.*⁵ within the standard tight-binding (TB) approximation. The gap opening process involves merging of two inequivalent Dirac points, \mathbf{D} and $-\mathbf{D}$.⁵⁻⁷ Such a process requires some $\sim 23\%$ of stretching along the zigzag chains⁵. The subsequent to Ref.5 and more realistic *ab-initio* calculations⁸⁻¹⁰ confirmed that the strain along a *zigzag* direction is indeed the most effective in annihilating the Dirac points. However, the ab-initio methods predicted even higher critical tensile strain ($\approx 27\%$) than that obtained within the tight-binding model. Moreover, it was discovered that annihilation of the Dirac points does not *automatically* lead to a gap opening, because a σ^* conduction band quickly moves down towards the Fermi level with the strain. As a result, when the Dirac points merge, the energy gap either does not open at all⁹, or opens by a tiny 45 meV¹⁰. Thus, the results^{5,9,10} suggest that a tangible gap in graphene is unlikely under uniaxial tensions up to the graphene failure strain of 25-27%^{2,4,11}. The papers^{5,8-10} considered a tension accompanied by a Poisson's contraction. Using a TB approach, Cocco *et al.*¹² have tried a uniform *pure shear* strain $\epsilon_{xy} = \epsilon_{yx} \neq 0$ associated with the elastic constant C_{44} . They claimed a moderate critical value of 16% and expected it to lower down to 12% if used along with the uniaxial strain in the armchair direction.

The idea of using inhomogeneous strain fields u with $\nabla_i u_k \neq 0$ has also been studied extensively bearing

on TB-derived notion of a pseudo-magnetic field $B \propto \nabla u$.¹³⁻¹⁵ It was claimed that two-dimensional corrugations with triangular symmetry open up a gap without a threshold¹³. The local gaps in graphene 'bubbles' have been reported in Ref. 14, while it was speculated that the one-dimensional corrugations ('wrinkles') that are frequently observed in a suspended graphene could open up the gap but only in combination with alternating electrostatic gating correlated with the 'wrinkles'¹⁵.

Here, we pursue two goals with the use of ab-initio calculations applied similarly to our earlier study of a flexoelectric [polarization induced by $\partial_x u_z \partial_y u_z$, $(\partial_x u_z \partial_y u_z)^2$ and $(\partial_x \partial_y u_z)^2$] 'sister' system B-N monolayer¹⁶. First, we show that contrary to Ref. 12 graphene's band structure remains gapless under *any uniform strains* not exceeding its breaking point. Secondly, we demonstrate that the energy gap can be nevertheless induced mechanically by applying realistic *nonuniform* sine-wave deformations (similar to the 'wrinkles') in all but the armchair directions, and *without* any periodic gating¹⁵. The qualitative difference with TB-derived continuous pseudo-magnetic models (see Ref. 15 and references therein) appears to be an account for strong $pp\sigma$ overlap between neighboring p_z orbitals on Carbon atoms appearing at any flexing with $\nabla u \neq 0$, in addition to the standard $pp\pi$ overlap, the only one retained in TB models of graphene. Since the rehybridization responsible for the gap opening is local, the results do not depend on standard procedure of employing supercell for the band structure calculations and atomic relaxation. Another feature missing in the continuous flexo-'magnetic' models is that they do not distinguish between flexing that is preserving an inversion symmetry versus a symmetry breaking one.

II. HOMOGENEOUS AND 1D PERIODIC DEFORMATIONS OF GRAPHENE

We begin with defining the homogeneous and inhomogeneous (sinusoidal) deformations of graphene. Select the unit vectors for real lattices of an undistorted

2D graphene as $\mathbf{a}_1 = \frac{a}{2}(\sqrt{3}, -1)$, $\mathbf{a}_2 = \frac{a}{2}(\sqrt{3}, 1)$ with the reciprocal lattice vectors $\mathbf{G}_1 = \frac{2\pi}{\sqrt{3}a}(1, -\sqrt{3})$, $\mathbf{G}_2 = \frac{2\pi}{\sqrt{3}a}(1, \sqrt{3})$. They are chosen in such a way that the x -axis is along the armchair direction ($\mathbf{a}_1 + \mathbf{a}_2$), while the y axis is along the zigzag direction ($-\mathbf{a}_1 + \mathbf{a}_2$). Let us consider a general homogeneous deformation of a graphene sheet. Excluding overall translation and rotations, such a change can be described by the displacements:

$$\begin{pmatrix} \delta x \\ \delta y \end{pmatrix} = \begin{pmatrix} \epsilon_0 + \eta & \gamma \\ \gamma & \epsilon_0 - \eta \end{pmatrix} \begin{pmatrix} x \\ y \end{pmatrix}, \quad (1)$$

where ϵ_0 corresponds to an isotropic distortion (dilatation), while the parameters η and γ describe the pure independent shear strains. By rotating the frame around the z axis through an angle ϕ given by $\cos(2\phi) = \eta/\sqrt{\eta^2 + \gamma^2}$, one can diagonalize the stress tensor in (1):

$$\begin{pmatrix} \delta x' \\ \delta y' \end{pmatrix} = \begin{pmatrix} \epsilon_0 + \tau & 0 \\ 0 & \epsilon_0 - \tau \end{pmatrix} \begin{pmatrix} x' \\ y' \end{pmatrix} \equiv \begin{pmatrix} \epsilon_{11} & 0 \\ 0 & \epsilon_{22} \end{pmatrix} \begin{pmatrix} x' \\ y' \end{pmatrix}, \quad (2)$$

where $\tau = \sqrt{\eta^2 + \gamma^2}$, $\epsilon_{11} = \epsilon_0 + \tau$ and $\epsilon_{22} = \epsilon_0 - \tau$.

For *inhomogeneous* deformations, it is sufficient to consider a periodic out-of-plane atomic displacements $u_z(\mathbf{r}) = A \sin(\mathbf{k} \cdot \mathbf{r} + \varphi)$, where \mathbf{k} is the undulation wave vector, \mathbf{r} is the in-plane vector with the origin at the lattice *inversion center*, and φ some phase. To set up the supercell calculations, we use a periodically and commensurately distorted graphene sheets, the corrugation wave vector is $\mathbf{k} = 2\pi\mathbf{e}/\lambda$, where the unit vector \mathbf{e} and the wavelength λ are given by $\mathbf{e} = \boldsymbol{\lambda}/\lambda$, $\boldsymbol{\lambda}(n, m) = n\mathbf{a}_1 + m\mathbf{a}_2$, $\lambda = a\sqrt{n^2 + nm + m^2}$, where n and m are integers, $|\mathbf{a}_1| = |\mathbf{a}_2| = a$, cf.^{17,18}. The corrugation with the period $\lambda(n, m)$ leads to a rectangular supercell with translational vectors $\boldsymbol{\lambda}(n, m)$ and $\mathbf{T} = N\mathbf{a}_1 + M\mathbf{a}_2$, $\mathbf{T} \perp \boldsymbol{\lambda}$, $N = (2m+n)/d_R$, $M = -(2n+m)/d_R$, where d_R is the greatest common divisor of $2m+n$ and $2n+m$.¹⁹ The number of graphene unit cells per supercell $\boldsymbol{\lambda} \times \mathbf{T}$ is $N_g = 2\lambda^2/(a^2 d_R)$.

For the undeformed graphene, the two inequivalent Dirac points are at $(2\mathbf{G}_1 + \mathbf{G}_2)/3$ and $(\mathbf{G}_1 + 2\mathbf{G}_2)/3$, respectively, at the two corners \mathbf{K} and \mathbf{K}' of the first Brillouin zone (BZ)⁷. It is easy to find the positions of these points inside the rectangular BZ of the supercell (when $A \rightarrow 0$) using a so-called zone-folding technique. Namely, $\mathbf{k} = 2\pi\mathbf{e}/\lambda$ is of one of the reciprocal vectors of the supercell, equal to $(-M\mathbf{G}_1 + N\mathbf{G}_2)/N_g$. The other reciprocal vector is $\mathbf{s} = (m\mathbf{G}_1 - n\mathbf{G}_2)/N_g$, and we find $\mathbf{K} = (2n+m)\mathbf{k}/3 + (2N+M)\mathbf{s}/3$, $\mathbf{K}' = (n+2m)\mathbf{k}/3 + (N+2M)\mathbf{s}/3$.¹⁹ In particular, for the corrugation along the zigzag direction with $\boldsymbol{\lambda} = (6, 0)$, both the \mathbf{K} and \mathbf{K}' points are translated into the origin (Γ -point).

The numerical calculations for both the flat and the corrugated graphene sheets have been performed using density functional theory implemented in the ABINIT

package²⁰. A $16 \times 16 \times 1$ Monkhorst-Pack \mathbf{k} -point grid²¹ has been used in the case of flat graphene. Approximately the same \mathbf{k} -point density was kept in going from the planar to a corrugated graphene. The sheets have been simulated by a slab-supercell approach with the inter-planar distances of $30a_B$ to ensure negligible wave function overlap between the replica sheets. For the plane-wave expansion of the valence and conduction band wave-functions, a cutoff energy was chosen to be 80 Ry. The plane waves Troullier-Martins²² and Fritz-Haber-Institute²³ pseudopotentials have been used for the calculations in the local density (LDA) and the generalized gradient (GGA) approximations, respectively. In both cases, Carbon 2s and 2p electrons have been considered as valence states.

III. NO GAP IN GRAPHENE SUBJECT TO A HOMOGENOUS DEFORMATION

Since any uniform strain respects the inversion symmetry, it can remove the Dirac point degeneracy only if it can force the Dirac points to merge, in compliance with the Wigner-von Neumann theorem. Merging may only take place at a point located at half the reciprocal lattice vector, $\mathbf{g}/2 = (p\mathbf{G}_1 + q\mathbf{G}_2)/2$, where p, q are integers⁷. Obviously, the Dirac point can be moved with regards to the reciprocal vectors only when the strain comprises the shear τ . Therefore, below we will distinguish three important cases of the *homogeneous* strain: (i) pure shear strain when $\epsilon_0 = 0$, $\epsilon_{11} = \tau$, $\epsilon_{22} = -\tau$ in (2), (ii) uniaxial tension accompanied by Poisson's transverse contraction, $\epsilon_0 = \tau(1+\sigma)(1-\sigma)$, $\epsilon_{22} = -\epsilon_{11}\sigma$, with σ the Poisson coefficient, and (iii) pure uniaxial tension ($\epsilon_0 = \tau$, $\epsilon_{11} = 2\tau$, $\epsilon_{22} = 0$).

We have performed detailed analysis with account for full atomic relaxation of the above cases (i)-(iii) exemplified by a graphene sheet under a tensile strain ϵ_{yy} with varying conditions for a perpendicular strain. In this geometry, the Dirac points merge in the case (i), when $\epsilon_{yy} = -\epsilon_{xx}$, and the strain ϵ_{yy} reaches 23.5%, while in the cases (ii) and (iii) for ϵ_{yy} exceeding 26.5 and 27.5%, respectively. Since the rate of σ^* -band lowering increases in passing from (iii) to (ii) and then from (ii) to (i), the gap is unable to open up in the cases (i),(ii) at all. Although the gap does open up in the case (iii), its maximal value is modest and does not exceed 100 meV since the antibonding σ^* -band quickly moves down in energy and closes the gap (see Fig. 1, cf.⁹). The suppressing role of σ^* -band can be traced back to the fact that the uniaxial strain changes the bond lengths and bond angles between C-C bonds along the stretching direction and perpendicular to it. The sp^2 hybrid tends to split into two sp_{\parallel} hybrids and the perpendicular to the stretching direction p_{\perp} chain states get progressively weaker coupled between themselves. As a result, the σ^* -band derived from p_{\perp} states quickly moves down at the point $\mathbf{k}/2$ ²⁴ thus fully suppressing the gap.

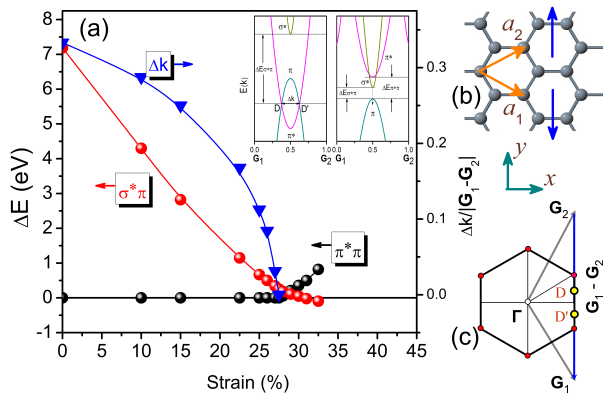


FIG. 1: (color online). ((a) The evolution of the gaps between the valence π and the conduction π^* and σ^* bands under uniaxial strain schematically shown in panel (b). The Dirac points move along the straight trajectory in BZ before merging (c). The bands along the merging direction from \mathbf{G}_1 to \mathbf{G}_2 are shown in the inset in (a) with the left (right) inset showing the bands before (after) the merging of Dirac points.

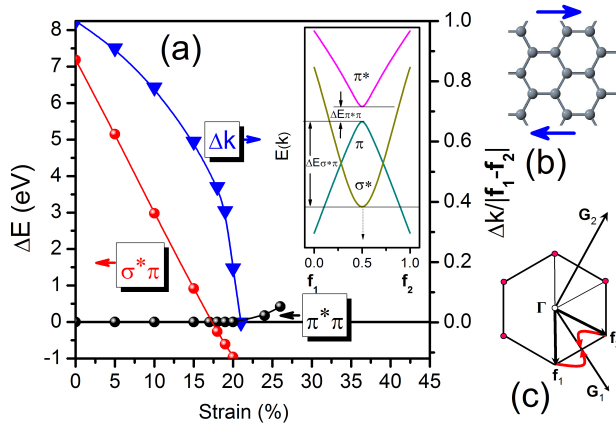


FIG. 2: (color online). (a) The evolution of the gaps between the valence π and the conduction π^* and σ^* bands under pure shear strain shown schematically in panel (b). The Dirac points move along complex trajectory in BZ before merging (c), where $\mathbf{f}_1 = (\mathbf{G}_1 - \mathbf{G}_2)/3$, $\mathbf{f}_2 = (2\mathbf{G}_1 + \mathbf{G}_2)/3$. The gap between π^* and π states opens up, but not before the $\sigma^* - \pi$ gap closes (inset in (a)).

The above results are obtained in the local density approximation (LDA) for the exchange-correlation energy. Using the generalized gradient approximation (GGA) instead does not change the results significantly, even though GGA usually favors gap opening. For instance, in the case (ii) GGA gives the critical value for the gap opening $\epsilon_{yy} = 25.3\%$ with the maximal gap value of about 100 meV. Keeping this in mind, below we present only the LDA results.

Scanning all possible deformations (i)-(iii) corresponding to different angles ϕ shows that the gap opening is

most problematic in the case of deformations involving stretching along the armchair directions. Here, the \mathbf{D} , \mathbf{D}' points should move the *longest* distance in \mathbf{k} -space to meet each other, and the latter can happen only well above the mechanical breaking strain. At the same time, the *pure shear* deformation conjugated to C_{44} elastic modulus ($\phi = \pi/4$, $\epsilon_{11} = -\epsilon_{22}$) was found to be the most favorable for the Dirac points merging, in agreement with Ref. 12. Evolution of the band structure under such a strain is shown in Fig. 2. In this case, the conduction σ^* -band minimum moves down (inset in Fig. 2a) and intercepts merging of two Dirac points when shear strain reaches 17%, while the merging occurs only when graphene sheet is strained by about 22%. One concludes that the homogeneous strain is unable to open up a gap in graphene, contrary to the claim in Ref. 12.

IV. GAP IN GRAPHENE SUBJECT TO TWO TYPES OF 1D CORRUGATION

Fortunately, the gap can be opened up in all but the armchair directions by the corrugation, with the maximal gap of about 0.5 eV for the zigzag direction. One can distinguish two qualitatively different regimes depending on a phase of the corrugation φ : (a) $\varphi = 0$, the inversion (and time reversal) symmetry is preserved, and (b) $\varphi \neq 0$, the inversion symmetry is generally broken. For the case (a), we have calculated corrugation along the zigzag direction $\boldsymbol{\lambda} = (6, 0)$, $\varphi = 0$ in Fig. 3. Such a perturbation is momentum dependent preserving time reversal and inversion symmetry and therefore can not automatically open up the gap in the graphene sheet²⁵ unless the Dirac points are merged at some point $\mathbf{g}/2$.⁷ In the case under consideration, the Dirac point moves on the symmetry $\Gamma - X$ line in the folded BZ, where $X = \mathbf{k}/2$, and ‘bounces’ off the X -point when A/λ is close to 0.12. Finally, the Dirac points merge at the Γ -point. The gap opens up when A/λ exceeds a critical value of 0.13 and quickly reaches a substantial size of 0.5 eV, as shown in Fig. 3 for $A/\lambda = 0.15$ (see also Fig. 6a). The wider maximal gap relative to the case of a stretched flat lattice is simply due to the fact that now the σ^* band is affected significantly less.

For possible applications, it is important to establish if the gap can be opened up when corrugation runs in a general *chiral direction* with an arbitrary phase φ . Band structure of graphene subject to a corrugation along a ‘chiral’ direction, $\boldsymbol{\lambda} = (-2, 3)$, $\varphi = 3\pi/19$, $A/\lambda = 0.14$ is shown in Fig. 4. Since $\varphi \neq 0$ and the inversion symmetry is broken, the gap opens up at any $A \neq 0$. However, the gap is very small if the ‘pseudo’ Dirac points remain well inside the BZ, which is the case for small corrugations. When the Dirac points approach the BZ boundary with increasing corrugation, the minimum of the conduction and the maximum of the valence band move apart in k -space. Consequently, the initially small gap grows to (indirect) gap of 0.5 eV, Fig. 4.

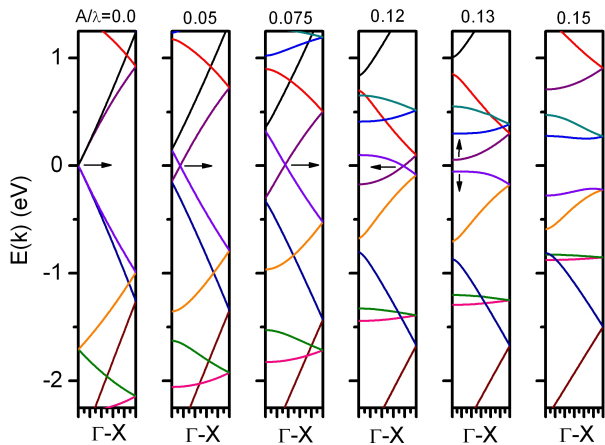


FIG. 3: (color online). Bands in graphene ($\Gamma - X$ direction) corrugated along the zigzag direction with $\lambda = (6, 0)$, amplitude to period ratio $A/\lambda = 0 - 0.15$ and the phase $\varphi = 0$ preserving the inversion symmetry. The Dirac points merge and the gap opens up when the corrugation is slightly smaller than $A/\lambda = 0.13$.

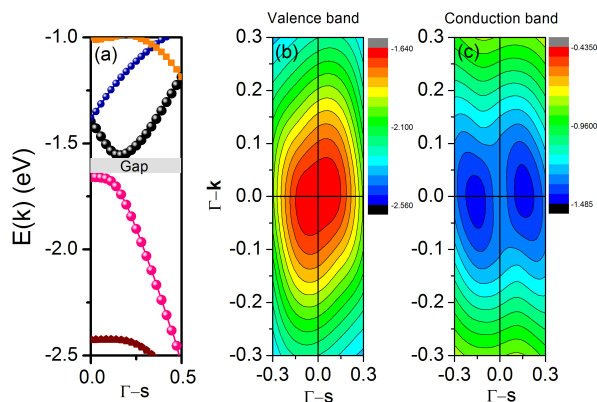


FIG. 4: (color online). (a) Gap in graphene corrugated along the chiral direction $\lambda = (-2, 3)$, with $A/\lambda = 0.14$ and the phase $\varphi = 3\pi/19$ breaking the inversion symmetry. The Dirac cones detach at $A \neq 0$ and after that their remainders evolve differently with corrugation forming the indirect gap (b),(c).

We should stress that in several aspects our results are in contrast with the gap behavior claimed on the basis of the continuous flexo-‘magnetic’ models^{15,26,27}. First, the latter are oblivious of the presence of the inversion symmetry or its lack thereof²⁶. As a result, they are missing the important increase in the gap size from trivially expected minute value in the symmetry-breaking case to large values when the remainders of the Dirac cones approach the BZ boundaries, Fig. 4. Second, even if the inversion symmetry is preserved, the gap can still open up when corrugation exceeds some limiting value. Such a gap opening does not require any periodic gating correlated with the corrugation suggested in¹⁵. And third,

it has been claimed that one-dimensional corrugations lead to creation of flat bands and a build up of the density of states (DOS) at the Dirac (neutral) point^{26,27}. These partially flat bands are believed to be analogs of the zero-energy Landau levels because the ripples affect the electrons like an effective magnetic field. Below, we show that in reality no flat bands occur since the Dirac points are stable up to the deformation where the system transforms into a metal.

As in Ref.26, we restrict ourselves to the limiting case of the armchair direction $\lambda = (n, n)$ with the inversion symmetry being preserved. Such a corrugation has a period of $2nb_0$, where $b_0 = \sqrt{3}a/2$ (the unit used in Ref. 26). When $A/\lambda = 0$, there are $2n$ conduction π^* bands and $2n$ valence π bands in the $\Gamma - X$ direction perpendicular to λ and containing a Dirac point (in the supercell BZ)¹⁷. Of these $2n$ bands (conduction or valence), two are nondegenerate and $n-1$ are doubly degenerate¹⁷. The π^* and π bands that form a Dirac cone are always nondegenerate (except for the Dirac point itself). When the corrugation is induced ($A/\lambda \neq 0$), all the doubly degenerate bands split due to breaking of the mirror symmetry. As A/λ is further increased, the lowest in energy split π^* band and the highest in energy split π band start moving toward the Fermi level, due to a change in the $\pi_z - \pi_z$ hopping matrix elements and increasing $\sigma^* - \pi^*$ and $\sigma - \pi$ hybridization.

To be more specific, consider the ripples with $n = 20$ and $\lambda = 40b_0$, Fig. 5. Here, the closest to the Dirac cone are the conduction and valence bands residing inside the Dirac cone almost symmetrically ($A/\lambda = 0$, Fig. 5). Such a relative position of the bands can be easily predicted by using the ‘band-folding’ procedure. As the A/λ increases, the degenerate π^* and π states split and repel each other, so that the lower/upper singly degenerate π^*/π state lowers/rises in energy. By approaching the Dirac cone, these two states considerably deform the latter. At some critical moment ($A/\lambda \approx 0.145$), the moving π^* and π bands reach the Fermi level leading to a peak in the DOS at the Fermi level (due to the evident van Hove singularities). In Ref. 26, this situation was interpreted as a formation of a flat pseudo-Landau level. In reality, however, we face here a peculiar *electronic topological transition* of the type semimetal-metal when the bottom of the π^* band and the top of the π band pass the Fermi level simultaneously. It is clear that such a transition is accompanied by electrons flowing from the π to the π^* band.

So far, we considered sine-wave deformations with only flexural (out-of-plane) atomic displacements. Such deformations are accompanied by the stretching $A^2k^2/4 = (\pi A/\lambda)^2$ which can be relieved by allowing the atoms to relax at a given amplitude A . ‘Annealing’ increases the initial quenched ratio A/λ because λ shrinks trying to restore the initial nearest-neighbor spacing. Since, on the other hand, the pace of movement of the Dirac points with A in the relaxed structures is slower, the critical corrugation $(A/\lambda)_c$ for the gap opening becomes consid-

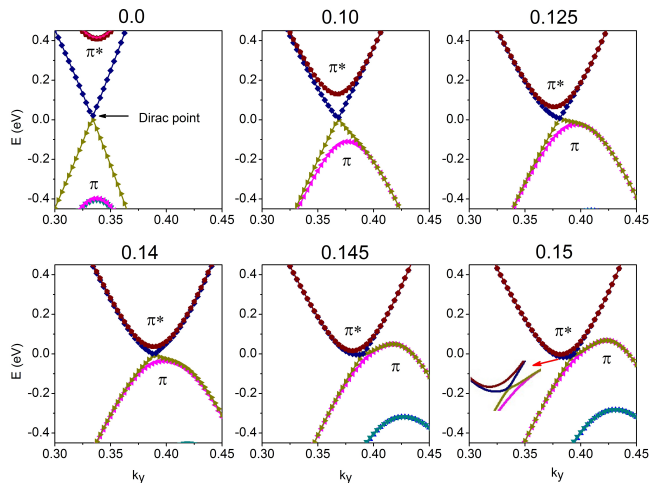


FIG. 5: (color online). Bands in graphene corrugated along the armchair direction with $\lambda = (20, 20)$, with amplitude to period ratio $A/\lambda = 0 - 0.15$ and the phase $\varphi = 0$ preserving the inversion symmetry. The k_y direction is perpendicular to the rippling direction. Note that the bands are defined in order of energy.

erably higher. For example, the annealing of the corrugated structure $\lambda = (6, 0)$ increases the critical corrugation from 0.12 to ~ 0.5 , Fig. 6a. It is important that in the relaxed structures, the σ^* band is affected significantly less than in the case of a stretched lattice and, therefore, one may open up a wider gap (~ 1 eV).

V. DISCUSSION AND CONCLUSIONS

It is clear from the above that the periodicity of the corrugations must not necessarily be commensurate with the undistorted graphene lattice or even sine-like for the gap opening. The commensurability between the deformation and the lattice itself would be important if the energy gap were due to mixing of electronic states belonging to two different valleys \mathbf{K} and \mathbf{K}' . However, in the case of 1D periodic corrugations this does not occur even if the corrugations provide a momentum transfer of $\mathbf{k} = \mathbf{K} - \mathbf{K}'$ (as in Fig.1) The gap opens only due to (i) breaking of the inversion symmetry and/or (ii) merging of two inequivalent Dirac points, as explained above. We simulated, for example, the situation when a corrugated graphene is placed on a hexagonal boron nitride (h-BN) and only a fraction of its atomic lines are in registry with h-BN. Such a partially coherent connection with the substrate maintains Gaussian-like periodic corrugations that we may call a ‘mesh’ (see the insert in Fig. 6b). In Fig. 6b, we present the results for a particular case when the graphene is deformed in such a way that its initial period $\lambda = (6, 0)$ becomes commensurate with the BN period $\lambda = (4, 0)$. We see that the corrugation leads to a gap of 0.20 eV. In practice, the periodic

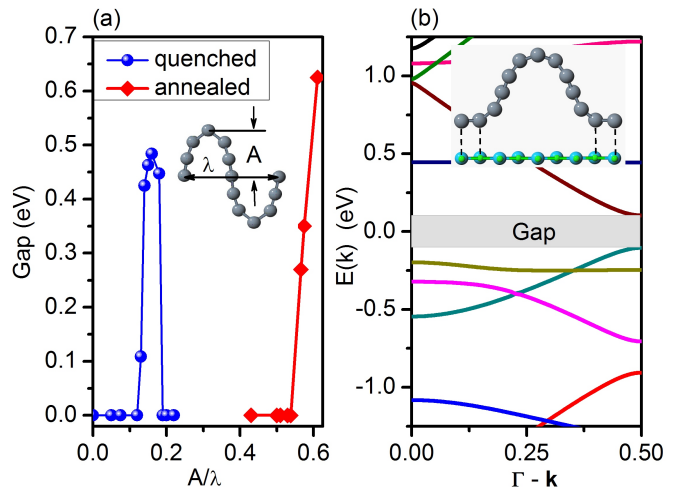


FIG. 6: (color online). Band gaps in corrugated periodic graphene sheets. (a) For quenched and annealed sinusoidal corrugations with $\lambda = (6, 0)$ as a function of the corrugation parameter A/λ . The critical corrugation $(A/\lambda)_c$ significantly increases in passing from the quenched to annealed ripple structures. The annealed structure at $(A/\lambda)_c$ is shown in the insert. (b) For a corrugated graphene placed on a hexagonal boron nitride (h-BN) substrate. It is supposed that the connection with the substrate is only partially coherent: within the period only four graphene atomic lines are in registry with h-BN lattice (shown by vertical dotted lines in the insert).

deformations can be achieved in various ways. One can imagine a situation when the edges are not clamped and a graphene membrane bends in accordion-like fashion. This situation corresponds to the ‘annealed’ corrugations where the initial nearest-neighbor lengths are mainly preserved. The ‘quenched’ corrugations can be induced by depositing graphene on a substrate like SiO_2 ²⁸ or the vicinal surfaces with regularly spaced steps, like $\text{Au}(788)$ ²⁹. In the case of SiO_2 , for example, the interaction energy between the graphene sheet and the substrate is sufficient to overcome the elastic energy needed for graphene to conform to the SiO_2 surface profile²⁸.

In conclusion, we have shown that any practical *homogeneous* deformation cannot open up a gap in graphene sheets. At the same time, the *inhomogeneous* deformation can open up a significant gap (~ 1 eV) rather independently of direction and form of a corrugation with an exception of an armchair direction. The present gap opening does not require any periodic gating correlated with the corrugation¹⁵ either. It is worth noting that in the limit of a clean undoped graphene sheet, the Coulomb interaction between electron and hole carriers may become significant if the Coulomb coupling constant exceeds some critical value on the order of unity and may facilitate an excitonic gap in the spectrum³⁰. However, in practical cases the Coulomb interaction may be screened by (unintentional) doping. Since a multilayer graphene (MLG)/graphite is a stack of weakly coupled graphene

sheets³¹, most of above results, therefore, should apply to the inhomogeneously deformed MLG as well.

-
- ¹ K. S. Novoselov, A. K. Geim, S. V. Morozov, D. Jiang, Y. Zhang, S. V. Dubonos, I. V. Grigorieva, and A. A. Firsov, *Science* **306**, 666 (2004).
- ² C. Lee, X. Wei, J. W. Kysar, and J. Hone, *Science* **321**, 385 (2008).
- ³ K. S. Kim, Y. Zhao, H. Jang, S. Y. Lee, J. M. Kim, K. S. Kim, J.-H. Ahn, P. Kim, J.-Y. Choi, and B. H. Hong, *Nature* **457**, 706 (2009).
- ⁴ F. Liu, P. Ming, and J. Li, *Phys. Rev. B* **76**, 064120 (2007).
- ⁵ V.M. Pereira, A.H. Castro Neto, N.M.R. Peres, *Phys. Rev. B* **80**, 045401 (2009).
- ⁶ P. Dietl, F. Piéchon, and G. Montambaux, *Phys. Rev. Lett.* **100**, 236405 (2008).
- ⁷ G. Montambaux, F. Piechon, J.-N. Fuchs, and M. O. Goerbig, *Phys. Rev. B* **80**, 153412 (2009).
- ⁸ Z. H. Ni, T. Yu, Y. H. Lu, Y. Y. Wang, Y. P.Feng, and Z. X. Shen, *ACS Nano* **2**, 2301 (2008).
- ⁹ Z. H. Ni, T. Yu, Y. H. Lu, Y. Y. Wang, Y. P.Feng, and Z. X. Shen, *ACS Nano* **3**, 483 (2009).
- ¹⁰ S.-M. Choi, S-H. Jhi, and Y.-W. Son, *Phys. Rev. B* **81**, 081407(R) (2010)
- ¹¹ E. Cadelano, P.L. Palla, S. Giordano, and L. Colombo, *Phys. Rev. Lett.* **102**, 235502 (2009).
- ¹² G. Cocco, E. Cadelano, and L. Colombo, *Phys. Rev. B* **81**, 241412(R) (2010).
- ¹³ F. Guinea, M. I. Katsnelson, and A. K. Geim, *Nat. Phys.* **6**, 30 (2010).
- ¹⁴ N. Levy, S. A. Burke, K. L. Meaker, M. Panlasigui, A. Zettl, F. Guinea, A. H. Castro Neto, and M. F. Crommie, *Science* **329**, 544 (2010).
- ¹⁵ T. Low, F. Guinea, and M. I. Katsnelson, *Phys. Rev. B* **83**, 195436 (2011).
- ¹⁶ I. Naumov, A. M. Bratkovsky, and V. Ranjan, *Phys. Rev. Lett.* **102**, 217601 (2009).
- ¹⁷ R. Saito, G. Dresselhaus, and M.S. Dresselhaus, *Physical Properties of Carbon Nanotubes* (Imperial College, London, 1998).
- ¹⁸ Results of the gap opening are not affected by this supercell approximation, as illustrated by gap opening in corrugated graphene partly attached to the BN substrate, Fig. 6b.
- ¹⁹ P. Marconcini and M. Macucci, *Carbon* **45**, 1018 (2007).
- ²⁰ X. Gonze *et al.*, *Comp. Mater. Sci.* **25**, 478 (2002).
- ²¹ H. J. Monkhorst and J. D. Pack, *Phys. Rev. B* **13**, 5188 (1976).
- ²² N. Troullier and J. L. Martins, *Phys. Rev. B* **43**, 1993 (1991).
- ²³ M. Fuchs and M. Scheffler, *Comput. Phys. Commun.* **119**, 67 (1999).
- ²⁴ W.A. Harrison, *Electronic Structure and the Properties of Solids* (Dover, 1989).
- ²⁵ J. L. Mañes, F. Guinea, and M. A. H. Vozmediano, *Phys. Rev. B* **75**, 155424 (2007).
- ²⁶ T. O. Wehling *et al.*, *Eur. Phys. Lett.* **84**, 17003 (2008).
- ²⁷ F. Guinea, M. I. Katsnelson, and M. A. H. Vozmediano, *Phys. Rev. B* **77**, 075422 (2008).
- ²⁸ M. Ishigami, J. H. Chen, W. G. Cullen, M. S. Fuhrer, and E. D. Williams, *Nano Lett.* **7**, 1643 (2007).
- ²⁹ N. Weiss *et al.*, *Phys. Rev. Lett.* **95**, 157204 (2005).
- ³⁰ D. V. Khveshchenko, *J. Phys. Condens. Matter* **21**, 075303 (2009).
- ³¹ Y. Kopelevich and P.Esquinazi, *Adv. Mater.* **19**, 4559 (2007).